中國機械工程學刊第二十五卷第三期第 267~276 頁(民國九十三年)
Journal of the Chinese Society of Mechanical Engineers, Vol.25, No.3, pp.267~276 (2004)

Development and Application of a Large Scale Fire Products Collector

Ming-Ju Tsai*, Chan-Wei Wu and Ching-Yuan Lin*****

Keywords: fire products collector, pool fire, heat release rate, oxygen consumption, motorcycle fire

ABSTRACT

A large-scale fire products collector is designed and fabricated, which is capable of analyzing a fire up to 10MW in heat release rate. Its design characteristics and applicability were tested by a gasoline-pool fire and a motorcycle fire. Their respective burning behaviors, fire products compositions, and heat release rates were recorded and recognized. In the pool fire tests, the heat release rate was computed from three available methods: CO and CO_2 generation, O_2 consumption, and gas temperature rise. By comparing the three calculated results with the heat release rate based on the mass loss rate determined by the load cell, the first two methods were found to give satisfactory data. In the motorcycle fire test, an ordinary 50c.c. motorcycle could reach a maximum heat release rate of 1.3MW, and was found to burn with more than one peak value of heat release rate because of the non-uniform distribution of its available flammable materials.

INTRODUCTION

The occurrence of fire is usually unexpected and disastrous. Reduction of life and property losses can only be achieved by extinguishing the fire in a shortest possible time. Thus, it is very urgent for fire-related researches to discover the cause, process and optimal extinguishing methods relevant to various types of fire. At present, the laws and regulations of fire protection in Taiwan are still under developed, therefore this study could be regarded as an important reference aiming at establishing a better standard to insure residential safety and environmental quality.

In the beginning of the 20th century, Thornton (1917) discovered that the heat release rate (HRR) per unit oxygen consumption was approximately constant (~13.1MJ/Kg-O_2) as organic liquids were burned. He reasoned that by utilizing the measurement of oxygen consumption, one could calculate the net heat release rate, which serves as an important indicator of the scale of a fire. Parker (1977) was the first researcher to utilize this principle in fire researches. Then Hugget (1980) found the above principle to be also suitable for organic solids. Based on oxygen consumption, the ideas of small heat release calorimeter gradually appeared. The first concept was devised by Smith (1971) in Ohio State University and subsequently the OSU calorimeter was developed.

The test procedure and calculation for a cone calorimeter were established according to the standards of ASTM E1354 (1999) and ISO 5660-1 (1999). By burning a specimen of material in this apparatus, one could appropriately record the physical changes and also measure the fire products, such as smoke, toxic gases and erosive substances. A small cone calorimeter can only evaluate quite small samples, e.g., the specimen cannot have a thickness larger than 50mm or contain jointed parts. Thus, for larger specimens, intermediate calorimeter (ICAL) has to be used and this equipment is specified in the standard ASTM E1623 (1999). In addition to cone calorimeters, fire products collector was also developed. Tewarson (1977) built a small-scale fire products collector of which the maximum HRR capacity was about 10kW. Since the fire scale is quite large in general, Heskestad (1981) developed a large-scale fire products collector which capacity could be extended to several mega-watts so that the behaviors of an actual fire could be simulated.

Paper Received January, 2004. Revised May, 2004. Accepted June ,2004. Author for Correspondence: Ming-Ju Tsai.

* *Architecture and Building Research Institute, Ministry of Interior, Tainan 711, Taiwan, ROC*
** *Department of Mechanical Engineering, National Cheng Kung University, Tainan 70101, Taiwan, ROC*
*** *Department of Architecture, National Taiwan University of Science and Technology,Taipei 106, Taiwan, R.O.C*

Several full-scale fire tests were conducted by NORDTEST, a joint Nordic organization for testing, from 1980 to 1990. A full-scale test is designed to represent a true fire so that its experimental results can hopefully be used to correlate other large fires. Sundström et al. (1987, 1988) tested the combustion of different objects in accordance with room-corner test regulated in ISO 9705 with ignition source described in the NORDTEST-method NT FIRE 025. The time for a fire to reach flash-over was the main consideration, and both smoke production and average production rates were also considered. There are five classes of fire were defined according to above -mentioned parameters.

Furnishings represent one of the bigger fire threats in homes and public buildings. The full-scale test based on NT FIRE 032 serves to assess the fire properties of a piece of furniture in case of a fire (Sundström, 1986). The test methods for curtains and draperies, developed in 1988 (Wetterlund et al., 1988), was intended for public buildings such as hotels, restaurants and theaters, not for dwellings. There are two main risks with curtains and draperies; one is the flame spread to be very rapid, which will involve a large burning area and quite a big heat release rate. The other main risk is that parts of the curtains may fall down and ignite other items such as upholstered chairs. This could lead to a very serious fire in a very short period of time. Babrauskas (1988) used combustion product collector to analyze HRR of various fuels and provided an empirical formula for mass consumption rate. In 1990, Kong et al. (1990) built a 1MW large-scale combustion analyzer system in Taiwan to study fire suppression of solid fuel arrays by water. In their study, wood frame structure was used to simulate the burning intensity of sofa in the research of Bill et al. (1989).

Early combustion product collectors have gradually become so-called cone calorimeters and there are about 140 small-scale sets around the world. In general, the data from small-scale fires cannot be extrapolated to larger-scale fires due to the variations in the phenomenon caused by the lack of dynamic similarity. As for large-scale fire products collector, only a few have been built in some places such as Underwriter Laboratory (UL) and Factory Mutual (FM) in the U.S. There are still huge gaps in extending our knowledge from small scale fires to large scale fires. The present paper describes the calibration of a 10MW large-scale fire products collector by gasoline pool fires. After determining the applicability of the apparatus, a motorcycle fire is tested.

EXPERIMENT SETUP

The large scale fire products collector is designed to analyze fire intensity up to 10MW. The system starts from a 7.62m×7.62m square collecting funnel, which is 10m above the ground, as shown in Fig.1, and ends with an exhaust gas scrubbing system and a suction fan, as shown in Fig. 2.

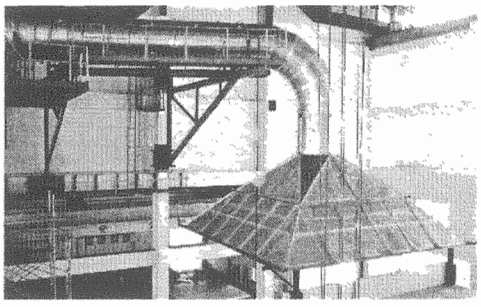

Fig. 1 Front end of the large scale fire products collector.

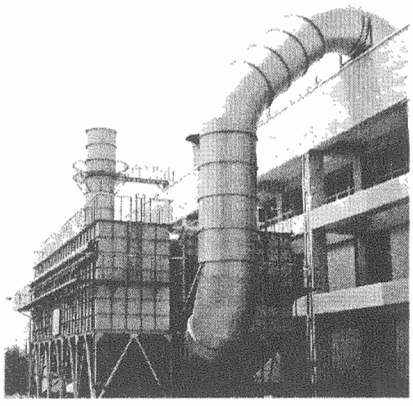

Fig. 2 Rear end of the large scale fire products collector.

The fire products gas flows into the collecting funnel due to the suction force created by the suction fan. Next, the gas flows through (1) a vertical pipe of inner diameter 1.524m, (2) a 90-degree bend which contains inner guide vanes to reduce secondary flows in the exhaust gas stream due to the bend, (3) an orifice plate of orifice diameter 0.896m, which serves as a mixing device, and (4) a long horizontal pipe made up of five pipe sections of length 1.524m each.

A schematic top view of the system is plotted in Fig. 3, which shows the relative positions of the various devices. To determine the smoke particles concentration in the fire products gas, a laser-based opacity detector is installed at cross section B. The main instrument station is set up at cross section A, which contains a pitot tube, a thermocouple, and a gas sampling pipe, for gas velocity, temperature, and composition measurement, respectively. On the pipe wall at cross section A, twelve 75mm dia. equally-spaced holes are drilled so that the various probes can be inserted through different angles. The definition of the angular coordinates can be seen in the D-D view.

The exhaust gas sample is fed into an on-line gas analysis system, which is capable of determining

the contents of O_2, CO, CO_2, NO_x and HC in the gas sample. All our sensing and measuring devices are consistent with those specified in ISO 9705, except that we use a pitot tube rather than a bi-directional probe for gas velocity measurement. We do not use the bi-directional probe prescribed by ISO 9705, because it is designed for a probe Reynolds number less than about 4000. In our system, we commonly operate at a probe Reynolds number greater than 8000, therefore only a pitot type probe is suitable in this situation. Downstream of the instrument station, a damper valve is provided for the control of the flow rate of the gas. The exhaust gas is cleaned in the gas scrubbing system and then flows out of the suction fan, which is controlled by a fan motor frequency converter, in which the maximum operational frequency is 55Hz, which corresponds to an exhaust rate of $30m^3/s$ in the large-scale fire products collector.

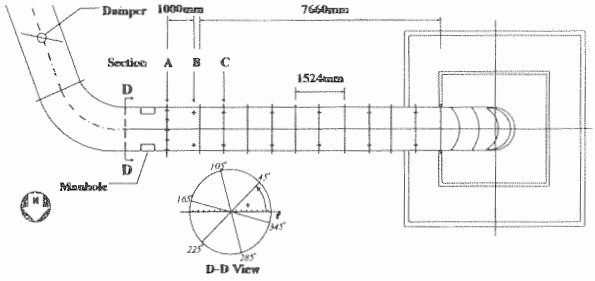

Fig. 3 Top view of the large scale fire products collector.

RESULTS AND DISCUSSIONS

A cold-flow velocity measurement was first conducted so as to realize the actual flow distribution and to determine an adequate position for flow rate measurement. A pool fire and a motorcycle fire were then used to test the stability and accuracy of the whole system.

Cold-flow Velocity Measurement

In Fig. 3 D-D view shows the angular coordinates. A pitot tube was inserted into the pipe along three radial directions (θ=45°-225°, 105°-285°, 165°-345°) to measure the velocity profile. In this experiment, the damper and the frequency converter could be used to control the amount of gas flow rate. The opening angle, α, of the damper valve could be adjusted in the range 0° ~90°, in which α=90° or 0° represents fully-open or fully-close respectively. For the frequency converter, the frequency, f, could be controlled from 0 Hz (fan stopped) to 55Hz (fan in full capacity).

Fig. 4 indicates gas speed versus radial position for various damper openings (α=30°, 60°, 90°), frequencies (f=10Hz, 20Hz) and angular positions (θ=45°-225°, 105°-285° and 165°-345°). The horizontal axis r/R represents the measuring radial position in relation to the pipe radius. r/R=0 is at the pipe center while r/R=1 is at the pipe wall. Left-hand-side r/R=1 represents pipe wall position at θ=105° (or 165°, 225°) while right-hand-side r/R=1 represents pipe wall position at θ=285° (or 345° and 45°). By referring to section D-D in Fig. 3, a general trend can be realized that the gas speed is slightly higher at the upper left (105°, 165° and 225°) part of the pipe cross section than at the lower right (285°, 345°, 45°) especially as f is increased. The reason is that the flow is slightly influenced by the elbow effect. In the downstream of the elbow following the collecting funnel, the velocity at the outer bend (θ=45°~105°) would rise owing to the centrifugal effect. And in approaching the elbow following the instrument station, the flow would also exhibit some acceleration phenomenon in the inner bend of the flow (θ=105° ~165°). The situation conforms to the description in Tananayev (1982).

Fig. 4 shows that at the same α and θ, velocity would increase as f increases; however, the velocity fluctuation would also increase. Taking α=30° for example, at f=10Hz, the velocity is around 2 m/s; at f=20Hz, the velocity is between 5 and 6 m/s, while the velocity distribution at f=10Hz is smoother than that at f=20Hz. If f is fixed, the velocity of the flow will rise as α increased from 30° to 90°. Besides, the distribution of flow is considerable uniform and the calculated location of the average velocity, which gives the volume rate of flow, sits near the center point (r/R=0). In the burning analysis, the pitot tube will be inserted from θ=345° and the velocity measuring position will be fixed at r=0 for the purpose of obtaining the volume rate of flow.

Heat Release Calibration

Gasoline Pool Fire Characteristics

After realizing the distribution of the flow field from cold-flow measurement, we proceed to calibrate the apparatus by actual burning. After considering the stability, flame type, heat release rate and smoke of the combustion, a pool fire is selected for the purpose of testing the proper functioning of the instrumentation on and evaluating the available heat release rate calculation methodology. The liquid-fuel pool is a 0.633m×0.633m standard stainless steel square vessel with a depth of 0.3m, which is mounted on a square frame with load cell. Water and gasoline are poured into the pool in sequence. The water is to stabilize the gasoline flame and to prevent the vessel from deformation.

In general, the heat release rate of a pool fire is dependent on the surface area of the pool. Hottel (1959) studied the relation between the pool area and heat release rate. On the amount of heat transfer, he concluded that, for a pool of diameter larger than 1m, radiation became the most important mode of heat transfer; thus the differences between large and small

pool fires are quite significant. Chatris et al. (2001) found that the burning history of a pool fire could be divided into three stages; namely, fire growth, fully development and burning-out period.

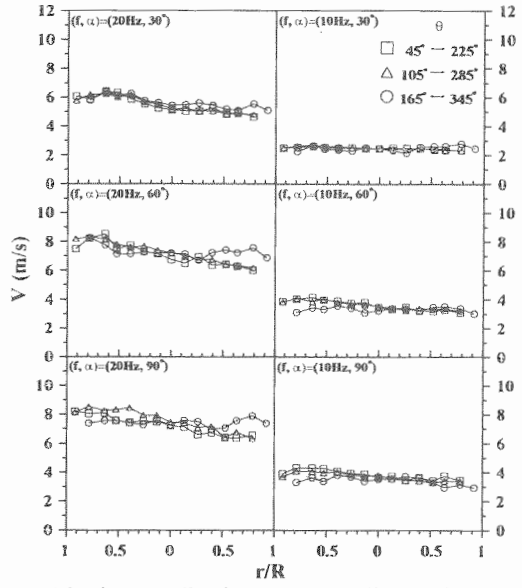

Fig. 4 Velocity distribution versus radial position for various damper openings, frequencies and angular positionS.

In our experiment, the vertical distance between the fuel pool and the collecting funnel is about 4.5m. The damper angle is set at $\alpha=90^{\circ}$ (fully open) and the velocity measuring position is at r=0 cm. Three calibration experiments with the amount of gasoline in fuel pool and its exhaust rate to be performed are: (1) 3500 c.c., 16kg/s, (2) 2500 c.c., 12kg/s, and (3) 2500 c.c., 8kg/s. The results are plotted in Figs. 5 and 6 where f indicates the frequency of suction fan converter. In principle, no matter how much gasoline is used, three stages of burning can be clearly seen as in the CO_2 plot in Fig. 5. Fire is gradually developing after ignition while CO_2 continuing to rise (t<50s), then CO_2 concentration remains nearly constant for a long period of time in the fully developed stage, and followed by a burn-out period with decreasing CO_2.

Figure 5 shows the compositions of pool fire products versus burning time. It is found that HC concentration in these three tests is quite stable. The variation of HC is between 12 and 8 ppm, this indicates that the combustion efficiency of the three conditions are quite similar. The basic trend for CO_2 and O_2 concentration is that CO_2 increases as O_2 decreases. In the figure, we see that O_2 displays a constant valley for a period of time, which shows the characteristic of steady combustion. As f is changed from 20Hz to 10Hz, the reduction in the concentration of O_2 is very apparent because induced air from inlet cone decreases. So the consumed O_2 represents a higher percentage of the combustion product gas. This can also be seen from CO_2 and CO concentration plots in which the reduced air flow causes CO and CO_2 concentrations to rise. Regarding to CO concentration, it shows that CO concentration gradually increases toward the end of burning. The reason is that as the pool fire grows, the burning intensity strengthens; heat transfer to the liquid pool will enhance vaporization of unburned-gasoline so that insufficient fresh air is entrained for complete combustion, and large quantity of unburned gas and smoke are produced.

Figure 6 shows the flow characteristics versus burning time. From the results, it can be realized that the flow distribution is still very smooth and the velocity and mass flow rate of the exhaust gas, V and $\dot{m}$, increase as f increases. The fan frequencies of 10Hz, 15Hz and 20Hz correspond to velocity of 4m/s, 6m/s and 8m/s respectively. Opacity mainly represents the visibility, which is inversely proportional to the amount of smoke in the exhaust gas. In the fully-developed burning period, opacity reaches 100%, which means total darkness without light penetration. The gas temperature T rises as the burning intensity increases. The plateau portion of the temperature curve is the characteristics of that the fully developed stage of pool fire, however, due to heat transfer to the pipe walls, the maximal temperature is established about 150s slower than the peak CO_2 concentration is. In the figure, we can also see that as the air velocity is reduced, the gas temperature goes up, but not beyond $60^{\circ}C$.

Heat Release Rate Calculation Methodology

The calculations of heat release rate of fires were developed in the past in three ways: (1) CO and CO_2 generation, (2) oxygen consumption, (3) gas temperature rise. For comparison, we briefly describe the three methods.

(1) CO and CO_2 Generation:

According to this method, the increment of mass flow rates of CO and CO_2, $\dot{m}_{CO}$ and $\dot{m}_{CO_2}$, in the exhaust should be measured and the heat release rate is found by

$$\dot{Q}_c = \Delta h_{CO_2}\dot{m}_{CO_2} + \Delta h_{CO}\dot{m}_{CO}. \qquad (1)$$

In this equation, $\dot{Q}_c$ denotes the heat release rate, while Δh_{CO_2} and Δh_{CO} respectively represent the combustion heat per kilogram of fuels converted into CO_2 and CO. In general, Δh_{CO_2} and Δh_{CO} are related to the fuel type; for gasoline fire, they are equal to 13.3 MJ/kg and 11.06 MJ/kg respectively.

(2) Oxygen Consumption:

In our experiment, water vapor is trapped before the gas sample reaches the gas analyzer and its O_2, CO_2, CO and HC concentration are measured. Since CO concentration in the combustion product is very low, it is suitable to use the equation of heat release

rate in ISO 9705. After the term of the continuous ignition source is taken out, the equation is shown as follows:

$$\dot{Q}_O = \Delta h_{O_2} \dot{m}_{O_2} x_{O_2}^a \left(\frac{\phi}{\phi(\gamma - 1) + 1} \right). \quad (2)$$

In equation (2), $\dot{Q}_O$ is the heat release rate; Δh_{O_2} is heat release per unit mass of oxygen consumed, and for gasoline, $\Delta h_{O_2} = 12.6$ MJ/kg; $\dot{m}_{O_2}$ is mass flow rate of O_2 in total fire products gas; ϕ is the oxygen depletion factor, $x_{O_2}^a$ is the ambient mole fraction of oxygen including water vapor and γ is the expansion factor due to chemical reaction. The details can be found in ISO 9705.

(3) Gas Temperature Rise:

$$\dot{Q}_T = \dot{m} C_p (T_g - T_o). \quad (3)$$

In this formula, $\dot{m}$, T_g and C_p are the total mass flow rate, temperature and specific heat of the fire products gas. T_o is the ambient temperature. For the yellow flame of a large-scale burning, this computation just represents the convective part of the combustion heat release, which is about 60~70% of total heat release.

By means of the above three methods, the heat release rate of the pool fire in the experiment can be determined and compared, and the results are plotted in Fig. 7. The results show that in the time period from 0 to 30 seconds, $\dot{Q}_C$ and $\dot{Q}_O$ rapidly increase from 0 to about 0.5MW and then reach approximately 0.6MW. This phenomenon can describe the initial development of the flame, in which there is a continuous increase in the size of flames and a progressive increase in the burning rate. As time proceeded from 50 to 300 seconds, the heat release rate oscillates for a period of time and then starts to decline. This rather stable period represents the fully developed fire with approximately constant burning rates. The duration of the fully developed fire is clearly a function of the amount of gasoline initially fed to the pool.

As time proceeds from 300 to 500 seconds, the flame gradually diminishes and then the burning intensity decays. This corresponds to the end of the fire, in which both the size of the flames and the burning rate decrease continuously until the extinction of the fire. At the final stage of the pool fire, the water below the gasoline may boil. Smoke may accompany steam and in the meanwhile the color of the smoke changes from black to white. Although the amount of gasoline is different, the three stages of the pool fire are still clearly recognizable. We can also see that heat release rate of a pool fire does not depend on the amount of liquid fuel in the pool. It is clearly shown in Fig. 7 that $\dot{Q}_O$ is equal to $\dot{Q}_C$ within 5% error.

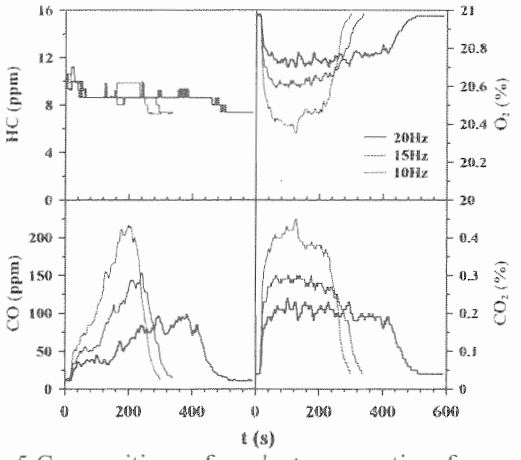

Fig. 5 Compositions of products versus time for pool fires.

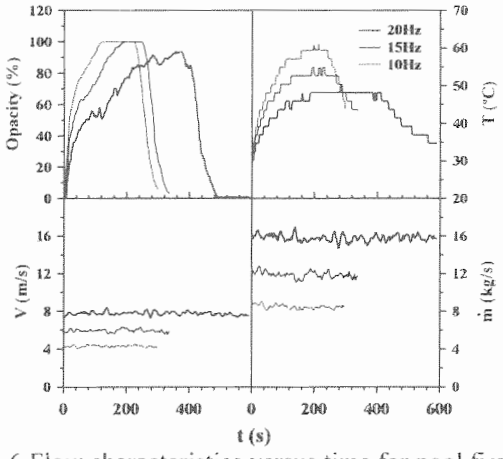

Fig. 6 Flow characteristics versus time for pool fires.

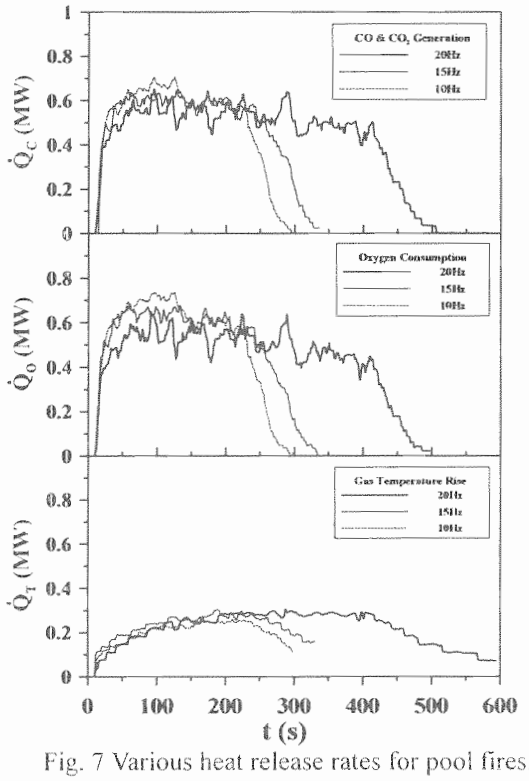

Fig. 7 Various heat release rates for pool fires.

Both methods give full account of the HRR. In the case of gas temperature rise method, it could be found that the value of $\dot{Q}_T$ is about 0.3MW which is much smaller than $\dot{Q}_C$ and $\dot{Q}_O$. The reason is that gas temperature rise method just takes into account the convective heat transfer but not including the heat loss due to radiation and conduction. Besides, the distance between the pool fire and the instrument station is long and not insulated, so heat loss to the surroundings cannot be ignored.

Mass Reduction Rate of the Pool Fire

To determine the accuracy of $\dot{Q}_C$ and $\dot{Q}_O$, liquid fuel mass reduction is recorded by load cells installed under the liquid-fuel pool. The results are shown in Fig. 8. Three straight lines are fitted to the data points which represented fully-developed fire stage. The slopes of the three lines are regarded as the mass reduction rates, $\dot{M}_{L,20Hz}$, $\dot{M}_{L,15Hz}$ and $\dot{M}_{L,10Hz}$ (kg/s). According to Babrauskas' research (1983), the theoretical mass reduction rate for a pool fire could be calculated by the following equation:

$$\dot{M}_L^T = \dot{M}_\infty (1 - e^{-k\beta D}) A, \tag{4}$$

where $\dot{M}_\infty$ is the mass reduction rate per unit area of an infinite diameter pool; $\dot{M}_L^T$ is the mass reduction rate; A is the pool area; D is the pool diameter; k is extinction-absorption coefficient and β is mean-beam-length corrector which differs for each fuels. For gasoline, $\dot{M}_\infty$ is 0.055 (kg/m^{2}s) and $k\beta$ is about 2.1 (m^{-1}). Inserting pool diameter D ~0.714m and area A ~0.4m^2 into Eq. (4), we obtained $\dot{M}_L^T$ ~ 0.0171kg/s. The heat release rate is then calculated by the following equation:

$$\dot{Q}_M^T = \dot{M}_L^T \times \Delta h, \tag{5}$$

where Δh is the combustion heat per unit mass of gasoline which is about 43.8MJ/kg. The theoretical heat release rate $\dot{Q}_M^T$ was then estimated to be 0.747MW.

The three load-cell experiments exhibit very similar values of mass reduction rate in the period of fully-developed burning stages, which are 0.0151, 0.0179 and 0.0170kg/s for 20Hz, 15Hz and 10Hz, respectively. After multiplying this value by the heating value of gasoline, 43.8MJ/kg, we obtain the heat release rate $\dot{Q}_M$ to be 0.661, 0.784 and 0.744 MW and the average value is about 0.73MW. The average error comparing with the theoretical heat release rate was within 5%.

By comparing the heat release rates $\dot{Q}_M$ with the heat release rates in Fig. 7, we can see that as the exhaust rate (fan frequency) is reduced, $\dot{Q}_C$ and $\dot{Q}_O$ approach more closely to $\dot{Q}_M \cong 0.73$ MW. $\dot{Q}_C$ and $\dot{Q}_O$ at 10Hz are about 0.7MW. The reason for this trend is that, as the exhaust rate is increased, the CO, CO_2, and O_2 concentrations in the exhaust gas become smaller and their measurements become less accurate. It is therefore concluded that, as long as the suction force is enough to collect the fire products gas, the exhaust rate should be kept to a minimum to raise the accuracy of concentration measurement.

The pictures of pool fire burning in the experiment were taken and shown in Fig. 9. These three photos represent three typical stages of the pool fire. For initial stage, the fire is just formed and the amount of the smoke is very limited as shown in Fig. 9(a). After a period of time, the fire becomes very strong and generates a great deal of black smoke as shown in Fig. 9(b). In this fully developed stage, the flame is high and the luminous radiation becomes quite noticeable. In the last stage, the fire transforms into a weaker fire and at this moment, a large quantity of water boils so that the smoke turns to white as shown in Fig. 9(c). The scale of fire is reduced gradually, and the flame burns out finally.

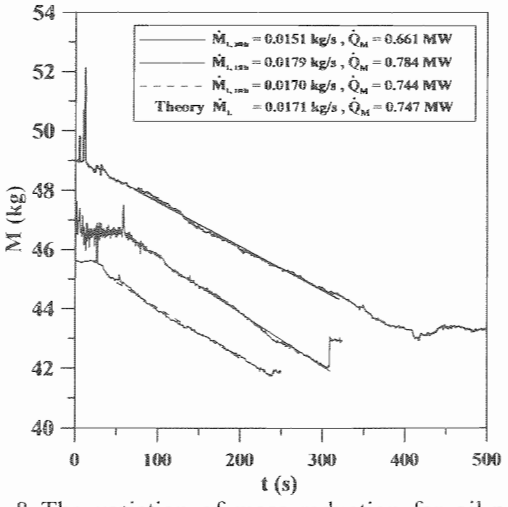

Fig. 8 The variation of mass reduction for oil-pool changes with time.

Heat Release Rate Calibration with 2 to 4 Gasoline Fire Pools

From the results of heat release rate of one oil-pool, it is found that oxygen consumption method is more accurate than the other two methods by comparing with actual mass reduction rate. Thus, in order to process larger heat release rate data, 2 to 4 oil-pools are used to calibrate heat release rate by oxygen consumption method and the results are shown in Fig.10. Each oil-pool is filled with the same amount of gasoline (6 liters) and water (72 liters) for the tests and exhaust rates were 20Hz, 20Hz and 30Hz for 2, 3 and 4 oil-pools, respectively. For a high heat release rate, a higher exhaust rate must be used

to take in the increased amount of fire product gas.

The results show that as the total area of oil-pool increase, the burning time would decrease owing to the increase of mass reduction rate. For 2-20Hz, 3-20Hz and 4-30Hz three experiments, the maximum heat release rate could reach about 1.75, 2.65 and 3.75MW respectively and the mass-reduction based heat release rate of the three cases are $\dot{Q}^T_{M,2\text{-}20} = 1.69$, $\dot{Q}^T_{M,3\text{-}20} = 2.67$ and $\dot{Q}^T_{M,4\text{-}30} = 3.65$ MW. Comparing these values, we can realize that the error is just within 5%.

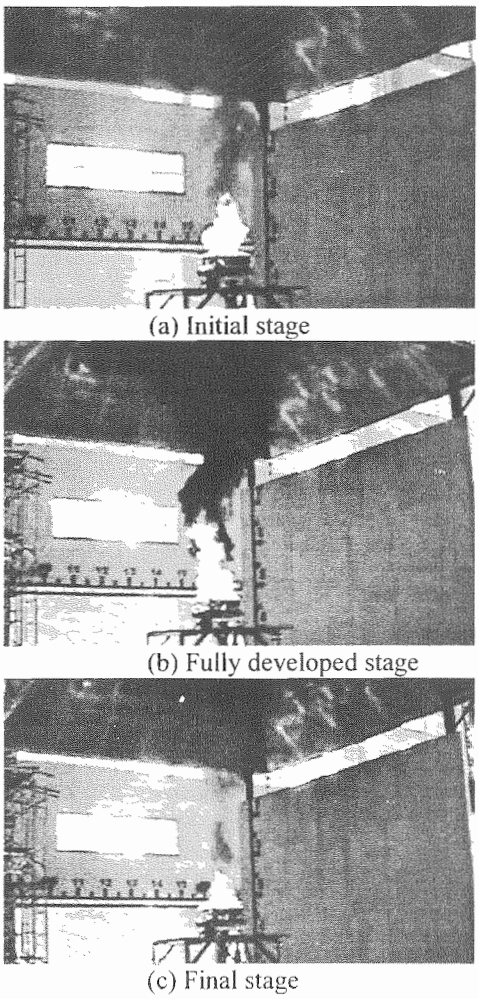

(a) Initial stage

(b) Fully developed stage

(c) Final stage

Fig. 9 Typical stages of a pool fire.

Motorcycle Test

After the pool fire test was done, the characteristics of the apparatus could be realized and the performances were found to be appropriate for heat release rate and combustion gas analysis, thus a motorcycle, which is a very common fire hazard in Taiwan, was selected to test its heat release and combustion characteristics. Since the motorcycle was a solid fuel and was hard to ignite, in this experiment an ignition source should be provided. Thus, a small gasoline pool of diameter 0.2m was set up under the motorcycle to ignite the motorcycle. The frequency f was set at 20Hz, which corresponded to an air mass flow rate of about 14kg/s and during the test, the compositions of exhaust, heat release rate and flow characteristics were all measured and calculated and then plotted in Figs. 11~13.

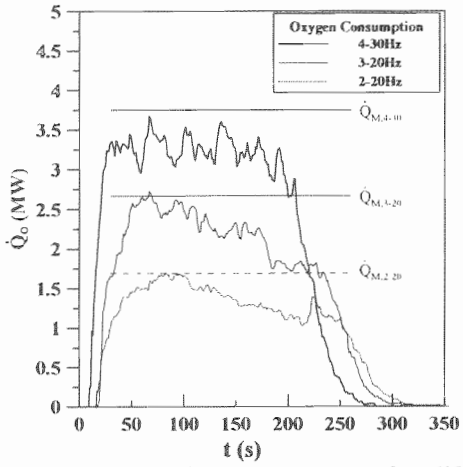

Fig. 10 Variation of heat release rate for different amounts of oil-pools.

Fig. 11 shows how the compositions of products vary as motorcycle burned. For O_2 and CO_2 concentration, they were complementary to each other, since very little CO production was produced. The concentration of O_2 had a minimum value of 20.2% at t=200s and became higher as time proceeded and meanwhile, the concentration of CO_2 had a maximum value of 0.5% and became lower as time proceeded. It could be seen that the combustion history for a motorcycle and a fuel pool was quite different. For a liquid fuel pool, owing to steady vaporization, a long period of fully-developed combustion is apparent. For solid fuel, however, it does not have a steady burning phenomenon, so the plateau zone in the O_2 and CO_2 curve for a pool fire could not be seen in Fig. 11. As for HC and CO concentrations, HC does not seem to vary noticeably and CO has a peak value when the combustion intensity is the largest. For a motorcycle, the plastic parts, such as the tires, seats, casing, handle,..., were the main type of fuel which could be burned and the exhaust contained many species especially dioxin and particles, which were very toxic and harmful to human beings. Figure 12 was the characteristics of the exhaust flow versus time as motorcycle burned. The opacity and temperature curves show one peak instead of a plateau portion. The maximal opacity reaches 95% around t=200s and the maximal temperature rise is 75℃ at t~300s. The peak temperature occurred 100s after the peak heat release because of heat transfer to the pipeline.

Figure 13 shows the three heat release rates computed by different analytical methods for the motorcycle fire. $\dot{Q}_C$ and $\dot{Q}_O$ are close and show a maximum heat release rate for the motorcycle at

about 1.2MW and $\dot{Q}_T$ is just 0.5MW. From t=0~100s, i.e. the beginning of fire, the heat release rate was about 0.12MW which represented the heat release rate of the ignition source, i.e. the 500c.c. of gasoline under the motorcycle. As the pool burned for about 100 seconds, the motorcycle was ignited and then kept burning; meanwhile, the pool gradually burned out. From the structure of a motorcycle, we can see that there are two major parts of available fuel: the front end and the rear end. Owing to the ignition of the pool fire closer to the front side of the motorcycle, the front part of the motorcycle burned first and then the fire extended to the center and rear part. Thus, it could be apparently found from the plots of the heat release rate, $\dot{Q}_C$ and $\dot{Q}_O$, that there was a smaller peak at t~500s.

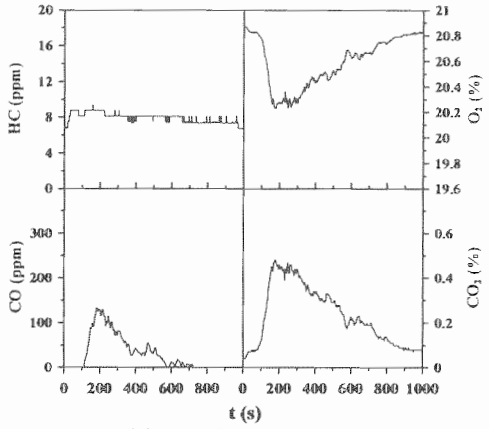

Fig. 11 Compositions of combustion products versus time for a motorcycle fire

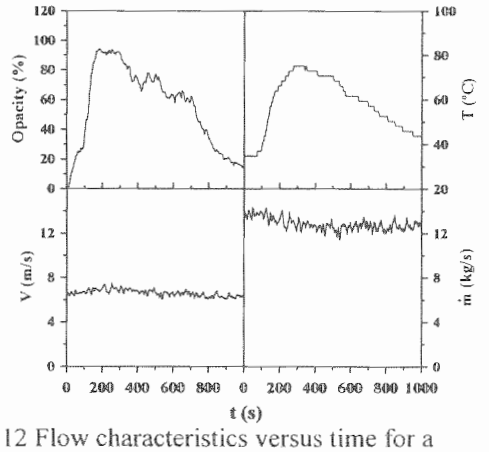

Fig. 12 Flow characteristics versus time for a motorcycle fire

Figure 14 displays the photos of the burning processes of the motorcycle fire. In Fig. 14(a), the appearance of the motorcycle and the gasoline pool location before burning could be seen. As the motorcycle burned, the fire intensity gradually became larger and the smoke was darker and bulkier than that of a pool fire. In Fig. 14(b)-(c), it could be seen that the front part of the motorcycle was burned first and then the fire extended to the rear part. During the combustion process, some unburned plastics would drop and then kept burning for a period of time. As the dropped plastic parts grew in quantity, the heat release rate would increase owing to the increase of the burning area, since the heat release rate is proportional to the surface area of the objects. After the burning of the motorcycle, only the metal frames remained and the flammable parts such as plastics and tires were all burned away entirely, as shown in Fig. 14(d). For a common 50c.c. motorcycle, the available mass of flammable materials is about 20kg.

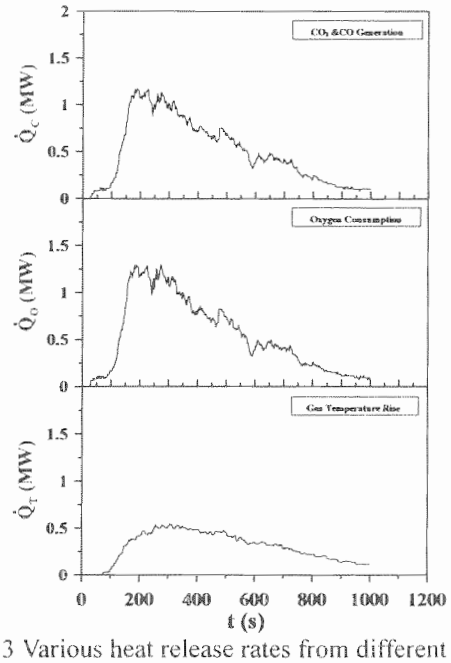

Fig. 13 Various heat release rates from different analytical methods for a motorcycle fire

CONCLUSIONS

In this study, a large-scale fire products collector was developed and calibrated up to 3.75MW. The combustion characteristics, heat release rate (HRR) of a pool fire and a motorcycle were tested. The performance of the fire products collector was found accurate and the conclusions are made as follows:

1. On the premise that the smoke could be collected completely, the exhaust rate should be kept to the minimum to enhance the precision of the concentration measurement and thus the heat release rate could be calculated more accurately.
2. CO and CO_2 generation, Oxygen consumption and gas temperature rise methods were used simultaneously to estimate HRR, the first two methods were found to give satisfactory data. However, oxygen consumption methodology was found to be the most accurate method for the calculation of heat release rate. And by comparison with the mass-reduction based heat release rate of a pool fire, the error was found to

be within 5%.

3. Variations of heat release rate in burning an ordinary 50 c.c. motorcycle showed that there is more than one peak value with a maximum of 1.3MW due to non-uniform fuel distribution.

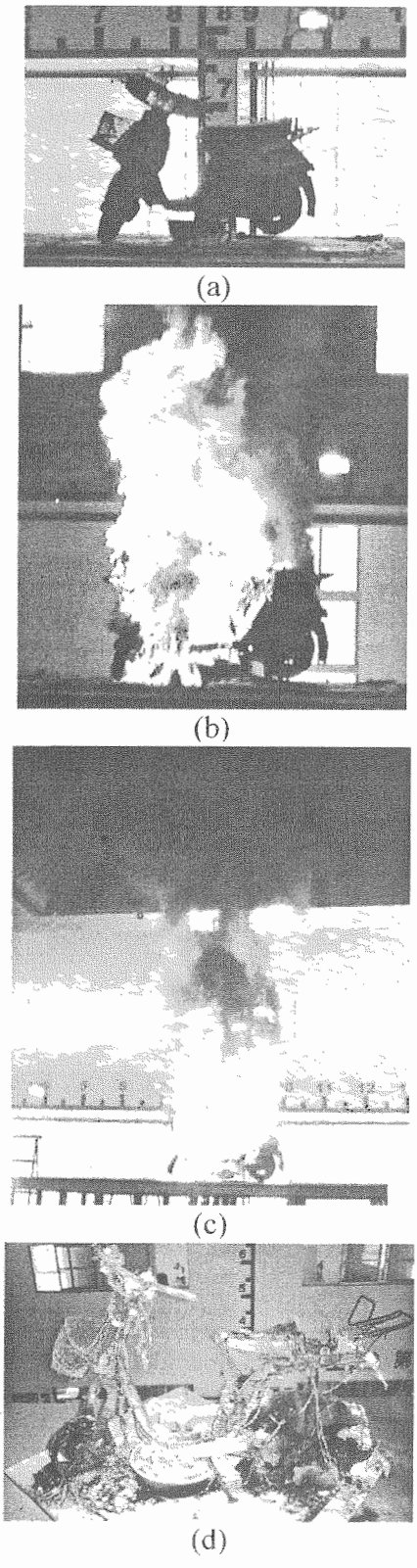

Fig. 14 Typical Stages of a motorcycle fire

REFERENCES

ASTM E1354, "Standard Test Method for Heat and Visible Smoke Release Rates For Materials and Products Using an Oxygen Consumption Calorimeter," ASTM Annual Book of Standards, Vol. 4.07, ASTM, West Conshohocken, PA, 1999.

ASTM E1623, "Standard Test Method for Determination of Fire and Thermal Parameters of Materials, Products, and Systems Using An Intermediate Scale Calorimeter (ICAL) ," ASTM Annual Book of Standards, Vol. 4.07, ASTM, West Conshohocken, PA, 1999.

Babrauskas, V., "Experimental Large Pool Fires of Burning Rate," Fire Tech. Vol. 19, pp. 251-261, 1983.

Babrauskas, V., "Burning Rate," the SFPE Handbook of Fire Protection Engineering, Chapter 11-1, National Fire Protection Association, Quincy, MA, 1988.

Bill, R.G., Jr., Brown, W.R., Hill, E.E., Jr., and Stavrianidis, P., "Sprinkler Research, Task 1: Fire Growth and Plume Measurements," FMRC Technical Report OQ5NO. RA070 (A), July, 1989.

Chatris, J.M., Quintela, J., Folch, J., Planas, E., Arnaldos, J., and Casal, J., "Experimental Study of Burning Rate in Hydrocarbon Pool Fires," Combustion and Flame, vol. 126, pp. 1373-1383, 2001.

Heskestad, G., "A Fire Product Collector for Calorimeter into MW Range," FMRE technical Report, June 1981.

Hottel, H.C., "Certain laws governing diffusive burning of liquids," Fire Research Abstracts and Reviews 1, pp. 41-44, 1959.

Hugget, C., "Estimation of Heat Release by Means of Oxygen Consumption Measurement," Journal of Fire and Materials, Vol. 4, No. 2, pp. 61-65 1980.

ISO 5660-1, "Fire Tests-Reaction to Fire-Rate of Heat Release from Building Products (Cone Calorimeter)," International Organization for Standardization, Geneva, Switzerland, 1993.

Kong, S.C., Chiou C.B., and Lin, T.H., "Fire Suppression of Solid Fuel Arrays by Water," NSC Report (Taiwan), NSC78-0401-E-006-08, 1990.

Parker, W.J., "An Investigation of the Fire Environment nment in the ASTM E-84 Tunnel Test," NBS Technical Note 945, 1977.

Smith, E.E., "An Experimental Determination of Combustibility," Fire Tech., Vol.7, p.109, 1971.

Sundström, B., "Full-Scale Fire Testing of Upholstered Furniture and the Use of Test Data," New Technology to Reduce Fire Losses and Costs, Elsevier Applied Science Publishers, 1986.

Sundström, B., "The New ISO Full Scale Fire Test Procedure for Surface Linings," The First Yugoslav Scientific Meeting with International Participation-On Behavior of Materials and Constructions in Fire, 1987.

Sundström, B. and Göransson, U., "Possible Fire Classification Criteria and their Implications for Surface Materials Tested in Full Scale According to ISO DP 9705/or NT FIRE 025," SP Report 1988:19, Statens provningsanstalt, Boras, 1988.

Tananayev, A.V., Gontsov, N.G., and Marinova, O.A., "Flow Structure in Pipe Elbows," Fluid Mechanic -Soviet Research, Vol.11, No.1, Jan.-Feb., 1982.

Tewarson, A., "Heat Release Rates from Burning Plastics," Journal of Fire and Flammability, Vol.8, p.115, 1977.

Thuillard, M., "A New Flame Detector Using the Latest Research on Flames and Fuzzy-Wavelet Algorithms," Fire Safety Journal, Vol. 37, pp. 371–380, 2002.

Thornton, W., "The Relation of Oxygen to the Heat of Combustion of Organic Compounds," Philosophical Magazine and J. of Science, Vol. 33, No. 196, 1917.

Wetterlund, I. and Göransson, U., "A Full Scale Fire Test Method for Free-Hanging Curtain and Drapery Textiles," SP-Report 1988:45, Swedish National Testing Institute, 1988.

NOMENCLATURE

A	surface area of pool (m^2)
C_p	constant pressure specific heat of air (kJ/kg-K)
D	pool diameter (m)
F	converter frequency of fan (Hz)
K	extinction-absorption coefficient
$\dot{M}_L^T$	theoretical mass reduction rate for a pool fire (kg/s)
$\dot{M}_{L,f}$	actual mass reduction rate of a pool for f=10, 15, 20Hz (kg/s)
$\dot{M}_\infty$	mass reduction rate per unit area of an infinite diameter pool (kg/m^2s)
$\dot{m}$	total mass flow rate of fire products gas (kg/s)
$\dot{m}_{CO}$	mass flow rate of CO in total fire products gas (kg/s)
$\dot{m}_{CO_2}$	mass flow rate of CO_2 in total fire products gas (kg/s)
$\dot{m}_{O_2}$	mass flow rate of O_2 in total fire products gas (kg/s)
$\dot{Q}_C$	heat release rate by using CO and CO_2 generation method (MW)
$\dot{Q}_M$	heat release rate by using mass reduction rate method (MW)
$\dot{Q}_M^T$	theoretical heat release rate by using theoretical mass reduction rate method (MW)
$\dot{Q}_O$	heat release rate by using O_2 consumption method (MW)
$\dot{Q}_T$	heat release rate by using gas temperature rise method (MW)
R	radial measuring position in cold flow field measurement (cm)
r/R	the ratio between radial measuring position and the radius of section area A
V	velocity of fire products gas in measuring section (m/s)
$x_{O_2}^a$	ambient mole fraction of oxygen including water vapor (%)
α	opening angle of damper (°)
β	mean-beam-length corrector
γ	expansion factor due to chemical reaction
Δh	combustion heat per kilogram of gasoline (MJ/kg)
Δh_{CO}	combustion heat per kilogram of fuels converted into CO (MJ/kg)
Δh_{CO_2}	combustion heat per kilogram of fuels converted into CO_2 (MJ/kg)
Δh_{O_2}	heat release per unit mass of oxygen consumed (MJ/kg)
θ	measuring angle of section A (°)
ϕ	oxygen depletion factor

大尺度燃燒產物收集器之發展與應用

蔡銘儒
內政部建築研究所
吳展維
國立成功大學機械工程學系
林慶元
國立台灣科技大學建築系

摘要

本研究主要建立一套熱釋放率達 10MW 之大尺度燃燒產物收集器，可用來模擬各種住宅單元、建築物與內裝材料等實際燃燒之情形，量測分析之數據可作為往後防火及相關法規訂定之參考。本文中，主要利用油盤穩定發熱之特性來進行本設備之效正，之後再以 50c.c.之機車來模擬實際火災發生之情形。本研究之熱釋放率計算主要利用三種方式：二氧化碳生成法、氧氣消耗法以及氣體升溫法，並在進行油盤燃燒時，同時針對其質量損失所得到之熱釋放率進行比較，結果發現，二氧化碳生成法及氧氣消耗法有較準確之結果。至於單部機車模擬試驗結果發現，隨著燃燒時間的進行，其熱釋放率則有數個峰值的現象，最大可達 1.3MW，主要可能是因為機車本身固體材料之非均勻分佈所造成的結果。